

# Studies of the Emitting States of Some Metalloporphyrins by Magnetically Induced Circular Emission (MCE)

R. A. Shatwell, R. Gale, A. J. McCaffery,\* and K. Sichel

*Contribution from the School of Molecular Sciences, University of Sussex, Brighton BN1 9QJ, Sussex, England. Received December 17, 1974*

**Abstract:** In this paper we describe the measurement of the magnetically induced circular emission (MCE) of a copper and palladium octaethylporphyrin at  $\sim 20$  K. This experiment yields the magnetic moments of the emitting states and these are interpreted using current theories. Uncertainties in the sample temperature prevent precise evaluation of the moments. However, results indicate that the emitting quartet in CuOEP experiences a strong Jahn-Teller distortion, and generally we find support for previous theoretical treatments of emitting states of diamagnetic and paramagnetic metalloporphyrins.

The electronic structure of the porphyrin ring system (Figure 1) has been the subject of intensive research in recent years and a wide variety of experimental techniques have been used to focus on this problem. In this paper, we describe the application of a new experimental technique to the study of porphyrins, namely the magnetically induced circular emission (MCE). Preliminary results have already been published using this technique.<sup>1</sup> Here we give a full description of the method applied to a study of the emitting states of some metalloporphyrins and illustrate the power of the technique in characterizing these states.

Many porphyrins phosphoresce from what is formally a triplet level in the red or near infrared region. This is spin forbidden from the ground state and as such has a low oscillator strength and long lifetime and is not seen in absorption. The small perturbations which the metal can induce may thus be responsible for order of magnitude changes in the radiative lifetime, and also radically affect the nonradiative decay to the ground state. Hence it is not surprising to find that the emission from porphyrin systems varies substantially with the nature of the metal substituent.<sup>2,3</sup>

In an attempt to investigate the effects of the metal atom on the magnetic moment of the phosphorescent level, two metal octaethylporphyrins (OEP) were studied at low temperature in polymer solutions. These were the palladium(II) compound, having a diamagnetic  $d^8$  metal atom, and the paramagnetic copper(II)  $d^9$  compound. The results for PdOEP are in agreement with existing theories, while those for the copper system indicate the presence of some unsuspected perturbations.

## Experimental Section

In a number of recent papers,<sup>1,4-7</sup> we have described measurements of magnetically induced circular emission (MCE) and the details of an earlier design of spectrometer employed in these experiments.<sup>5</sup> Since this represents a new form of emission spectroscopy, we give here a full description of the technique and the information to be obtained from its use.

The optical components in this experiment are shown in Figure 2. The sample is mounted in a longitudinal magnetic field and is excited by a monochromatic light source. In some cases this was a 500 W xenon arc lamp focussed on the entrance slit of a Spex "Minimate" monochromator (Mc 1 in Figure 2). For most results reported here, however, the 5145 Å line of a Spectra Physics 4 W argon ion laser was used. Here the "Minimate" functioned to remove the numerous plasma lines which would otherwise be superimposed on the spectra. In order to attain low temperatures and high magnetic fields, the samples were mounted in the bore of a superconducting magnet and fields of up to 18 kG were available. Sample temperatures were measured with the aid of a carbon resistance thermometer. The optical components before the sample

in Figure 2 allow the selection of different forms of polarization of exciting radiation; linear, circular, or effectively depolarized. This last function will be described shortly.

If the emitting state of the excited molecule is degenerate the magnetic field separates the Zeeman components and the circular polarization of emission reflects the relative populations of the Zeeman components. If spin-lattice relaxation is fast, and this will generally be the case for the temperatures used here (23 K was the lowest measured temperature), we can assume a Boltzmann distribution across the Zeeman components. The degree of circular polarization, expressed as a fraction of the total emitted radiation, is a function of the absolute temperature and of the magnitude of the Zeeman splitting. Thus a measurement of the circular polarization of emission for a known sample temperature enables the magnetic moment of the emitting state to be evaluated. In circumstances where spin-lattice relaxation is sufficiently slow that thermalization of the  $M_J$  components does not take place during the lifetime of the state, quite different relations will govern the emission polarization. Studies of this kind on porphyrins at temperatures below 4.2 K will be the subject of further communications. A simple test of the validity of our assumptions concerning a Boltzmann distribution across the Zeeman components is available through the temperature dependence of circular polarization. This should show  $1/T$  dependence; as does the Faraday  $C$  term in the analogous MCD experiment.<sup>8</sup> In the case of PdOEP this relation was found to hold within the range 23–65 K and this observation provides good indication of rapid thermalization.

The circular polarization of the emitted radiation is analyzed by a photoelastic modulator (pem in Figure 2) followed by a linear polarizer ( $P_2$ ). These convert the polarization information to an intensity modulation of the component transmitted by  $P_2$ . The radiation is wavelength analyzed by a Spex 1406 double grating monochromator and detected by an EMI 9558 QB photomultiplier. Two signals are generated in the photomultiplier anode load: one an ac current periodic with the modulator (50 kHz); the other a dc current which measures the total emitted light intensity. The former signal is detected by a phase-sensitive detector (psd) referenced at the modulation frequency and provides a measure of the circular polarization in the form  $(I_+ - I_-)$  (see ref 7 for details). The dc signal is proportional to the function  $(I_+ + I_-)$  and is amplified by a Keithley picoammeter. Both signals are fed to separate channels of a dual-pen chart recorder for simultaneous display. Two other features of the instrument deserve mention. In cases where signal enhancement is needed, the output may be coupled to a Varian CAT and the instrument programmed for automatic repetitive scanning. Another valuable feature is a servo device which may be used to maintain a constant dc anode current and thus make measurements of circular polarization *ratio* for varying light intensities. We also add here that this same instrument is suitable for use in a variety of optical experiments including Raman spectroscopy and magnetic circular dichroism.

The palladium octaethylporphyrin was prepared using the method described by Falk.<sup>9</sup> It was dissolved in vacuum distilled methyl methacrylate and placed in sealed ampoules. The solutions were polymerized by heating in an oven at 80° using the remaining oxy-

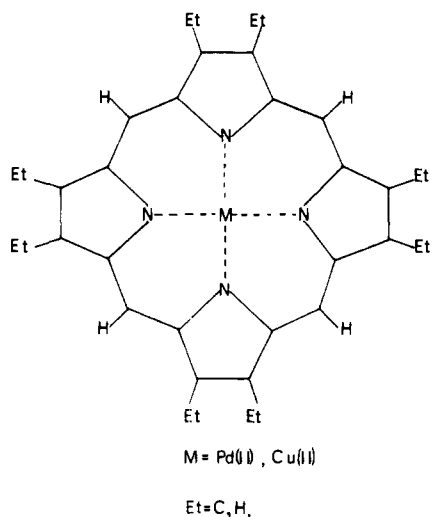


Figure 1. The octaethylporphyrin skeleton M = Pd(II) or Cu(II).

gen in the ampoules as an initiator. Solutions of CuOEP in polystyrene were prepared in a similar manner using samples of metalloporphyrin kindly donated by Professor A. W. Johnson and Dr. P. Batten. Following polymerization the samples were cut on a diamond saw to thin, parallel-sided disks for mounting in the cryostat. The optical surfaces were polished to reduce depolarization and scatter and any sample-induced depolarization of transmitted radiation was always less than 3%. Typical optical densities of the resultant disks were around 0.2 for the  $Q_{0-0}$  transition. This is roughly equivalent to concentrations of the order of  $4 \times 10^{-5}$  mol l<sup>-1</sup>.

Sample temperatures during the experiment were monitored by a carbon resistance thermometer, the probe being cemented into a small hole drilled in the sample. The sample was cooled by contact with the bore of the superconducting magnet cryostat and the minimum temperature reached was a surprisingly high 23 K. This was presumably due to the poor conductivity of the polymer host. The sample temperature could be raised by increasing the laser power although this effect was generally minimized by using low laser intensities and dilute samples.

The metalloporphyrins are highly anisotropic absorbers and hence if polarized light is used to excite them in a rigid medium, the emission will be partly polarized due to photoselection.<sup>10</sup> Laser radiation is highly polarized and large zero-field base lines result from its use as an excitation source. It is difficult to depolarize the radiation completely, so a method was adopted in which the nature of the incident polarization was constantly changed. If in a time interval comparable with, or less than, the response time of the measuring system (i.e., the time constant of the psd) the polarization averages to zero, then no resultant zero-field signal will be recorded. In practice a second photoelastic modulator, adjusted to give half-wave retardation, was placed between the Glan-Thompson laser polarizer and the sample. This had an effective "rotation" frequency of 100 kHz and proved quite satisfactory. Careful measurements of the MCE signal obtained in this manner, and those obtained using linear or circularly polarized laser radiation and subtracting any zero-field base line, showed all three signals to be identical within experimental error.

The emission spectra we report compare favorably with those obtained by Gouterman et al.<sup>11</sup> Excitation spectra taken by scanning with a narrow-band, monochromated xenon source indicated that the major absorbing species were also responsible for emission. The spectra were interpreted using moments techniques. A brief review of the theory relevant to porphyrins is given in the Appendix. The expressions are essentially similar to those of Henry et al.<sup>12</sup> and Stephens<sup>13</sup> but differ slightly since here we deal with spontaneous emission rather than with absorption.

### Theory

In order to discuss the experimental results it is necessary to give a brief review of the current state of theory and experiment concerning the porphyrins. The basis of the theory was first outlined by Gouterman.<sup>14</sup> The spectra in the visi-

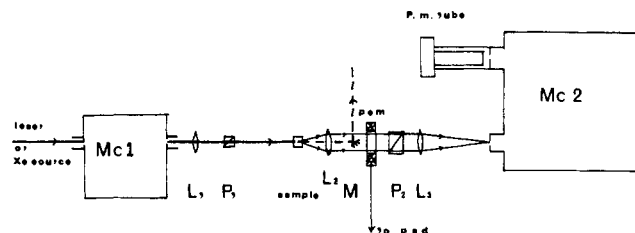


Figure 2. Schematic diagram of MCE apparatus.

ble and near-uv regions arise from transitions within the  $\pi$  electron system. Simple LCAO-MO theory gives the two highest occupied orbitals the symmetries  $a_{1u}$  and  $a_{2u}$ . Two 1-electron  $\pi$ - $\pi$  excitations can then take place to an unoccupied doubly degenerate  $e_g$  orbital:  $a_{1u} \rightarrow e_g$  and  $a_{2u} \rightarrow e_g$ . This gives rise to two degenerate singlet and two degenerate triplet states of  $E_u$  symmetry. The  $^1E_u$  states mix heavily by configuration interaction, giving a visible band with low oscillator strength and high magnetic moment (the Q bands) and a uv band (Soret) with the converse properties. Configuration interaction within the triplet manifold is forbidden group theoretically.<sup>15</sup>

This model needs to be refined slightly to account for the slight shifts in band positions, and oscillator strengths, with metal substituent. The  $a_{2u}$  orbital may interact with the p orbitals of the metal, lifting the degeneracy of the pure configuration states, and hence altering the extent to which configuration interaction takes place. Ring substituents also have an effect on the energies of the 1-electron orbitals. Thus in the octaalkylporphyrins the  $|({}^2a_{1u})({}^2e_g)^3E_u\rangle$  should lie lower than  $|({}^2a_{2u})({}^2e_g)^3E_u\rangle$ . The situation is reversed in the tetraphenyl porphyrins.<sup>14</sup>

Work by Sutherland et al.<sup>16</sup> on the MCD and Zeeman effect of the  $Q_{0-0}$  band of zinc coproporphyrin indicates the presence of a zero-field splitting of this state. These conclusions are supported by the work of Gradyushko<sup>17</sup> and van der Waals et al.<sup>18</sup> on porphyrins in *n*-octane lattices. The latter authors interpret their results in terms of a Jahn-Teller interaction coupled with a low-symmetry distortion induced by the lattice. Sutherland showed that the MCD of these states was relatively insensitive to any zero-field splittings, but nevertheless gave good values for the magnetic moments (this conclusion may also be arrived at directly from the moments theory for MCD interpretation).

The foregoing refers to metalloporphyrins having closed shell, diamagnetic metal atoms. An extensive theoretical treatment of the paramagnetic porphyrins and the diamagnetic  $d^8$  systems was undertaken by Ake.<sup>15,19</sup> The basis for Ake's model was the idea put forward by Murrell<sup>20</sup> to explain the quenching of the benzene emission by paramagnetic molecules such as oxygen. It is assumed that the metal d orbitals are coupled to the  $\pi$  system of the ring by a weak exchange interaction. In CuOEP this gives rise to  ${}^2E_u$  and  ${}^4E_u$  states having approximately the energies of the old  ${}^3E_u$ , with the  ${}^2E_u$  states approximately 100 cm<sup>-1</sup> higher in energy than the quartet band. Electric dipole transitions from the "trip-doublet",  ${}^2E_u$ , state to the ground state ( ${}^2B_{1g}$ ) are now weakly allowed, whereas the oscillator strength for the "trip-quartet" is much less and arises through spin-orbit coupling with allowed doublet levels. The variable temperature and lifetime measurements of Gouterman et al. give some support for this model.<sup>11,21</sup>

Similar ideas are used to describe the  $d^8$  systems. Here, the singlet and triplet states seen in absorption and emission have the same form as those for the closed shell metalloporphyrins, but the nonradiative decay to the ground state is strongly affected by the presence of extra levels, arising from the coupling of paramagnetic excited states on the

metal with the ring orbitals. Again, the experimental work by Gouterman and coworkers is consistent with Ake's theoretical deductions.<sup>19</sup>

### Results and Interpretation

The results for palladium octaethylporphyrin will be discussed first, since these are in closest agreement with existing theories. The spectra are shown in Figure 3. The emission spectrum consists of an intense band origin at 6600 Å followed by relatively weak transitions to vibrational levels of the ground state extending to beyond 8000 Å. The MCE spectrum is all of one sign and roughly mirrors the emission line shape except for a few regions in the vibronic side bands. These will be discussed later. For the moment attention will be concentrated on the band origin and its associated MCE.

According to Ake the phosphorescent level is a  ${}^3E_u$  level formed by excitation from  $a_{1u} \rightarrow e_g$  on the porphyrin ring, combined with an unexcited  ${}^1a_{1g}$  metal orbital. The form of the wave functions may be derived using the methods of Griffith,<sup>22</sup> or by standard MO techniques. They are:

$$\begin{aligned} |({}^1a_{1g})({}^2a_{1u}){}^3E_u \pm 1, +1\rangle = \\ |{}^2a_{1u}\tau, +\frac{1}{2}\rangle |{}^2e_g \pm 1, +\frac{1}{2}\rangle |({}^1a_{1g})({}^2e_g){}^3E_u \pm 1, 0\rangle = \\ \frac{1}{2^{1/2}} \{ |{}^2a_{1u}\tau, +\frac{1}{2}\rangle |{}^2e_g \pm 1, -\frac{1}{2}\rangle + |{}^2a_{1u}\tau, -\frac{1}{2}\rangle \times \\ |{}^2e_g \pm 1, +\frac{1}{2}\rangle \} |({}^1a_{1g})({}^2a_{1u})({}^2e_g){}^3E_u \pm 1, -1\rangle = \\ |{}^2a_{1u}\tau, -\frac{1}{2}\rangle |{}^3e_g \pm 1, -\frac{1}{2}\rangle \quad (1) \end{aligned}$$

Here the first number in the parentheses refers to the orbital component, the second to the  $M_s$  value. The superscript refers to spin multiplicity. We have chosen to express the orbital components in the complex coordinate scheme given by Griffith, rather than in the real cartesian system. Thus the states are diagonal in the operator  $L_z$ . This has the advantage of making the rotational averaging of the moments expressions simpler, and further the states are generally more convenient to deal with when treating the interaction with circularly polarized light.

The ground state of the molecule is  $|{}^1A_{1g}\rangle$

$$|{}^1A_{1g}\rangle = |{}^2a_{1u}\tau - \frac{1}{2}\rangle |{}^2a_{1u}\tau, +\frac{1}{2}\rangle \quad (2)$$

and hence transitions are spin forbidden from the triplet state. Oscillator strength can be obtained by spin-orbit mixing with allowed levels. In the  $D_{4h}$  symmetry group, the spin-orbit coupling operator may be expressed as a double tensor operator of the form:<sup>22</sup>

$$\bar{1} \cdot \bar{s} = (1s)_0^2 |{}^1_0\rangle + (1s)_{-1}^E |{}^1_{+1}\rangle + (1s)_{+1}^E |{}^1_{-1}\rangle \quad (3)$$

The first term on the rhs connects the  ${}^3E$  state with allowed  ${}^1E$  states. From the nature of this term, it is clear that it will only bring oscillator strength into the  $M_s = 0$  component of the triplet, and that the coupling will be diagonal in the orbital quantum number, i.e.,

$$\begin{aligned} \langle {}^3E\gamma M_s | (1s)_0^2 | {}^1E_\gamma 10\rangle = \\ (-1)^{1-M_s} \delta_{\gamma\gamma'} \langle {}^3E | (1s)^{A_{21}} | {}^1E\rangle V(E_\gamma^E, E_{\gamma'}^A) \bar{V}({}^1_{-M_s}, 0 | 0) \quad (4) \end{aligned}$$

The other terms in (3) could mix possible singlet charge transfer states with the  $M_s \pm 1$  levels of  ${}^3E$ . However, it would be expected that this would give these levels a different oscillator strength from the  $M_s = 0$  component, resulting in a double exponential form for the decay curve in zero field. This is not found to be the case,<sup>10</sup> so such contributions will be neglected here. The model adopted considers mixing with the  ${}^1E$ ,  $Q_{0-0}$  band (or, indeed, any other  ${}^1E$  level), giving oscillator strength only to transitions from the  $M_s = 0$  components of the triplet.

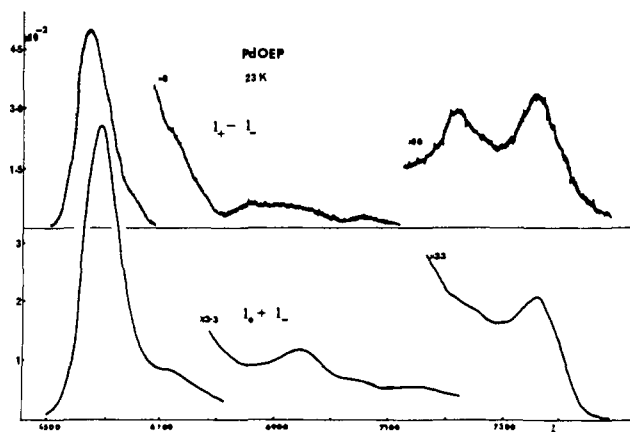


Figure 3. The emission spectrum and MCE of PdOEP in poly(methyl methacrylate) at 23 K in a field of 17.8 kG. The intensity scales are arbitrary and are uncorrected for instrument response. However, the scales are calibrated relative to one another and this is shown.

Additional justification for this assumption comes from the phosphorescence polarization experiments of Gurinovich et al.<sup>23</sup> who have observed linear polarization ratios,  $\rho$ , of  $1/2$  for some metalloporphyrins.

Working on these assumptions, the expression for the zeroth moment of emission is (see Appendix)

$$\langle \bar{F}_0 \rangle = \frac{-\beta H_z}{2kT} \frac{i}{2^{1/2}} \langle E \| L \| E \rangle \quad (5)$$

The calculated value of  $\langle F_0 \rangle$  at a measured  $T = 23$  K and a field of 17.8 kG is  $-0.054$ . Since the moments expressions in the Appendix are defined in terms of  $I_+ - I_-$  rather than the opposite way round, as in absorption, and since the field is in the opposite direction from the absorption experiments, this still gives the zeroth moment a negative value when expressed in the sign convention common to absorption MCD studies.

The sign of the splitting may be established in other ways, however. As mentioned above, the spin-orbit coupling between singlet and triplet is diagonal in the orbital quantum number. Thus transitions from the ground state to a  $|{}^3E, \gamma, 0\rangle$  level should have the same polarization as those transitions to a  $|{}^1E, \gamma, 0\rangle$  state. The  $g$  factors for both singlet and triplet should also have the same sign if the wave functions in eq 1 accurately represent the triplet state. It ought to be possible, therefore, to establish the sign of the emission "C" term from the absorption "A" terms. The works of Stephens et al.<sup>24</sup> and Gale et al.<sup>25</sup> both indicate that the "A" term for the  $Q_{0-0}$  transition has a negative lobe at low energy. This would give rise to a negative "C" term in fluorescence, which should have the same sign as the phosphorescence MCE, as is the case.<sup>1</sup>

Substitution of the parameter values into (5) gives

$$\langle E \| L \| E \rangle = -2.9i \quad (6)$$

The one-electron reduced matrix element may be deduced from eq 1. It is the same:

$$\langle e \| l \| e \rangle = -2.9i$$

The matrix element  $\langle e_{gy} | l_z | e_{gx} \rangle$  is then given by

$$\langle e_{gy} | l_z | e_{gx} \rangle = -\frac{1}{2^{1/2}} \langle e \| l \| e \rangle = 2.1i \quad (7)$$

This value is in remarkably close agreement with that calculated by McHugh et al.<sup>26</sup> These authors obtained 2.09*i* in a SCMO calculation. The result is somewhat lower than was obtained by Stephens or by Dratz<sup>27</sup> from the MCD of zinc coproporphyrin on the related singlet states,

Table I. The Vibrational Structure of PdOEP

Designation <sup>a,b</sup>	Wavelength, Å	Energy, cm <sup>-1</sup>	Distance from 0-0, cm <sup>-1</sup>
0-0	6606	15136	
$\nu_1$	6726	14866	270
$\nu_2$	6933	14423	713 (b) <sup>c</sup>
$\nu_3$	7133	14019	1117
$\nu_4$	7233	13825	1311 (a <sub>2</sub> ) <sup>c</sup>
$\nu_5$	7367	13575	1561 (a <sub>1</sub> ) <sup>c</sup>
$\nu_6$	7533	13274	1862

<sup>a</sup> $\nu_4, \nu_5$  show pronounced MCE. <sup>b</sup> $\nu_2$  has no discernible MCE signal. <sup>c</sup>Tentative vibrational assignments from the work of Nestor and Spiro (ref 24).

though these are expected to be influenced by extensive configuration interaction. The closeness of this value to theoretical should be viewed with some degree of caution however. It is likely that the excited molecules are not in thermal equilibrium with the polymer "bath" and their temperature may well be higher than the measured 23 K. The value in eq 7 represents a lowest estimate of the orbital *g* factor therefore.

Figure 3 also shows the vibronic side bands and their associated MCE. Table I gives their designation and approximate positions and energies. The intensities of the side bands are very low in comparison to the band origin, and are, for the most part, ill-defined and broad. The same remarks apply also to the MCE. This for the most part follows the emission profile and is the same sign as the band origin, although there is a possible negative going peak at around 6820 Å. The bands  $\nu_4$  and  $\nu_5$ , shown amplified, have a more pronounced MCE than the rest. The  $\nu_5$  peak is at approximately 1500 cm<sup>-1</sup> from the band origin, around the same distance as the Q<sub>0-1</sub> band is from the Q<sub>0-0</sub> in absorption. This strongly suggests that  $\nu_5$  is associated with the "a<sub>1</sub>" vibration which is the most prominent contributor to the Q<sub>0-1</sub> band. In Table I we give the tentative vibrational assignments from the Raman data of Nestor and Spiro.<sup>28</sup> It is apparent from these that the a symmetry vibrational structure shows appreciable MCE while those of b symmetry do not. A vibronic calculation shows the a symmetry features to have the same sign MCE as the origin while those with b symmetry will have opposite signs. For the most part, the vibronic structure is not sufficiently well defined to merit detailed analysis at this stage.

Perhaps the most important conclusion to be drawn from a study of the vibronic side bands is that their intensity relative to the band origin indicates that the <sup>3</sup>E potential energy well is almost vertically above that of the ground state. This will have an important bearing on the study of the CuOEP emission, to be discussed below.

Gouterman<sup>11</sup> investigated the variation of quantum yields and lifetimes of a variety of copper-porphyrin systems with temperature. He found that the quantum yield goes down with decreasing temperature below about 60 K. Also the lifetime decay curve is nonexponential and may be decomposed into a short and a long decay time. The results were interpreted in terms of Ake's model<sup>19,21</sup> involving a doublet level approximately 100 cm<sup>-1</sup> above a quartet state, and a thermal equilibrium existing between them. A kinetic scheme was evolved expressing quantum yields and lifetimes in terms of the rate constants for various radiative and nonradiative processes. More will be said of this later. For the moment, the compatibility of Ake's theoretical predictions with the observed MCE will be investigated.

The emission spectrum and MCE of CuOEP, as functions of laser power, are shown in Figures 4-7. If it is assumed that the variation with laser power is equivalent to a

variation in temperature, then the emission spectrum closely parallels the published ones of Gouterman et al.<sup>11</sup> The carbon resistor probe was relatively insensitive to changes in laser power, so information on the actual temperature at which the spectra were taken is not forthcoming. The MCE at low power consists of a negative going peak underneath a possible band origin at 6912 Å. As the temperature is raised a band appears at higher energy, 6820 Å, which is more intense and has an opposite sign MCE associated with it, obscuring the original signal. There is no evidence of any MCE underneath the vibronic side bands, despite these being more intense than the 6912 Å transition at low laser power.

According to Ake's theory, the <sup>2</sup>E<sub>u</sub> and <sup>4</sup>E<sub>u</sub> wave functions may be generated by coupling the unperturbed porphyrin <sup>3</sup>E<sub>u</sub> states, given in eq 1, to the <sup>2</sup>b<sub>1g</sub> state on the copper atom. When a complex basis set is used, this gives:

doublets

$$|({}^2b_{1g})({}^2a_{1u})({}^2e_g){}^2E_u \pm 1, +\frac{1}{2}\rangle = \frac{1}{6^{1/2}} \{2|{}^2b_{1g} - \frac{1}{2}\rangle |{}^2a_{1u} + \frac{1}{2}\rangle |{}^2e_{1g} \mp 1, +\frac{1}{2}\rangle - |{}^2b_{1g} + \frac{1}{2}\rangle |{}^2a_{1u} + \frac{1}{2}\rangle |{}^2e_g \mp 1, -\frac{1}{2}\rangle - |{}^2b_{1g} + \frac{1}{2}\rangle |{}^2a_{1u} - \frac{1}{2}\rangle |{}^2e_g \mp 1 + \frac{1}{2}\rangle\} \quad (8a)$$

and similarly for the  $|{}^2E_u \pm 1, -\frac{1}{2}\rangle$  states, and

quartets

$$|({}^2b_{1g})({}^2a_{1u})({}^2e_g){}^4E \pm 1 + \frac{3}{2}\rangle = |{}^2b_{1g} + \frac{1}{2}\rangle |{}^2a_{1u} + \frac{1}{2}\rangle |{}^2e_g \mp 1, +\frac{1}{2}\rangle |{}^2b_{1g} - \frac{1}{2}\rangle |{}^2a_{1u} - \frac{1}{2}\rangle |{}^2e_g \mp 1, +\frac{1}{2}\rangle = \frac{1}{3^{1/2}} \{(|{}^2b_{1g} - \frac{1}{2}\rangle |{}^2a_{1u} + \frac{1}{2}\rangle |{}^2e_g \mp 1, +\frac{1}{2}\rangle + |{}^2b_{1g} + \frac{1}{2}\rangle |{}^2a_{1u} + \frac{1}{2}\rangle |{}^2e_g \mp 1, -\frac{1}{2}\rangle + |{}^2b_{1g} + \frac{1}{2}\rangle |{}^2a_{1u} - \frac{1}{2}\rangle |{}^2e_g \mp 1, +\frac{1}{2}\rangle\} \quad (8b)$$

and similarly for the  $|{}^4E \pm 1, -\frac{1}{2}\rangle$  and  $|{}^4E \pm 1, -\frac{3}{2}\rangle$  states. These agree with Ake's functions defined in the real basis set.

First-order spin-orbit coupling splits the  $M_s = \pm\frac{3}{2}$  levels apart by an amount  $\pm z/2$ , while the  $M_s = \pm\frac{1}{2}$  levels of the quartet are split by  $\pm z/6$ . The doublet  $M_s = \pm\frac{1}{2}$  levels are separated by  $\pm z/3$ . *z* is estimated to be between 3 and 20 cm<sup>-1</sup>.<sup>8</sup> A magnetic field removes the degeneracy completely. The level splitting, together with the polarization of the allowed transitions, is shown in Figure 8. The factors *z* and *K* are proportional to the reduced matrix elements for spin-orbit coupling and magnetic-field splitting:

$$z = \frac{-i}{3^{1/2}} \langle e_g || (1s)^{a_2} || e_g \rangle$$

$$K = \frac{i}{2^{1/2}} \langle e_g || (1)^{a_2} || e_g \rangle \quad (9)$$

For comparison, an indication of the splitting of the  $|{}^3E \pm 10\rangle$  levels of PdOEP is also provided in Figure 8. The polarizations of the transitions were calculated by assuming spin-orbit coupling between the  $|{}^4E \pm 1, \pm\frac{1}{2}\rangle$  levels and allowed  $|{}^2E\rangle$  states. As with PdOEP, this coupling is diagonal in  $M_s$  and the orbital quantum number. The nature of the splitting of the  $M_s = \pm\frac{3}{2}$  levels has been left out of Figure 8 for clarity. These terms mix with allowed doublets through the last two elements of the spin-orbit coupling operator in (3). If these operations are performed it can be shown that those levels with energy  $+z/2$  are allowed in *z* polarization, and hence may contribute to the emission intensity but not to the MCE [eq 16, Appendix]; transitions from the levels with energy  $-z/2$  are forbidden (see also work by

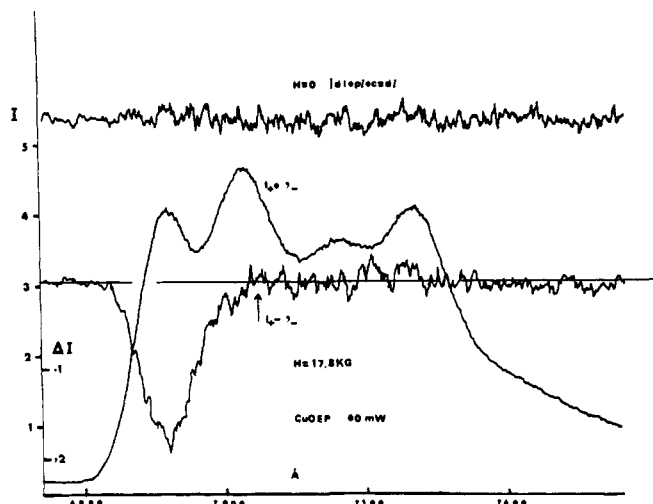


Figure 4. Emission spectrum and MCE of CuOEP in poly(methyl methacrylate) at low temperature in a 17.8 kG field. Laser power 40 mW.

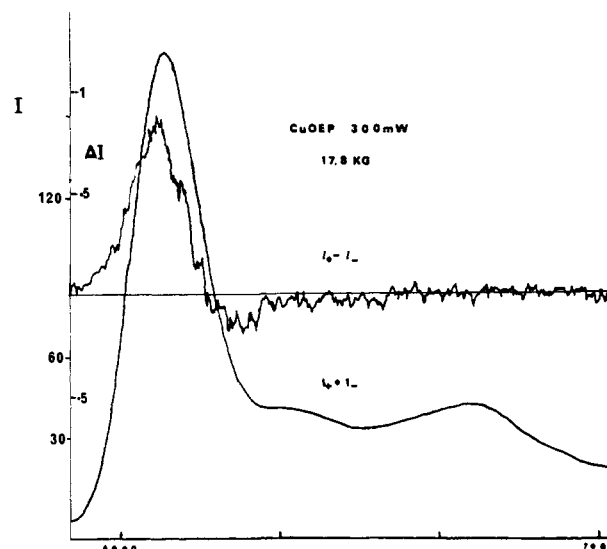


Figure 7. As for Figure 4 but with 300 mW laser power.

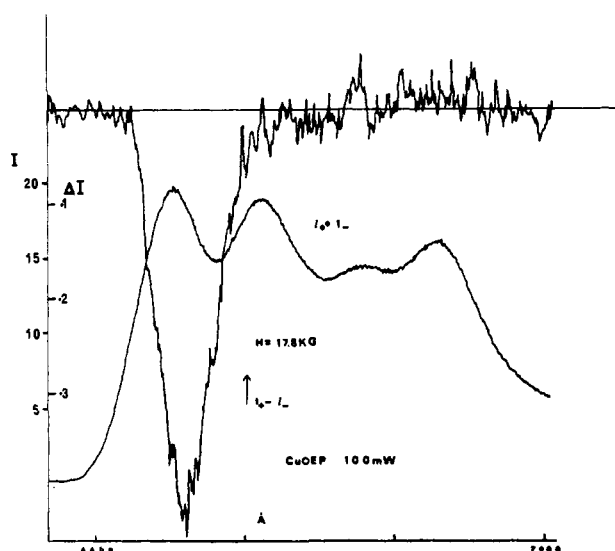


Figure 5. As for Figure 4 but with 100 mW laser power.

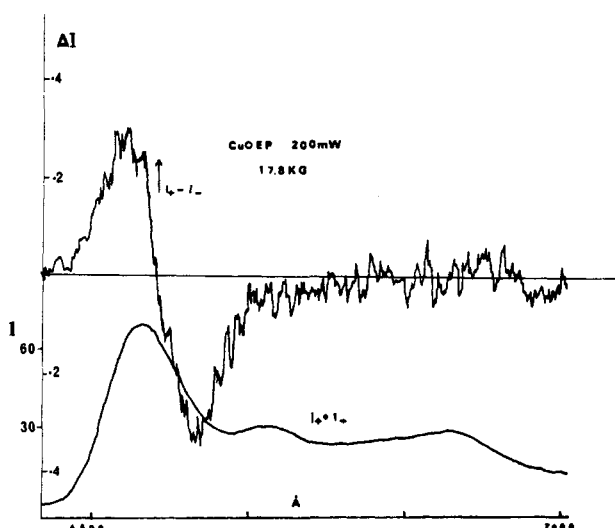


Figure 6. As for Figure 4 but with 200 mW laser power.

Ake).<sup>15,19</sup> The oscillator strengths of the z polarized transitions would be expected to be much smaller than those with  $P = \pm 1$ , since the doublet levels are much further away.

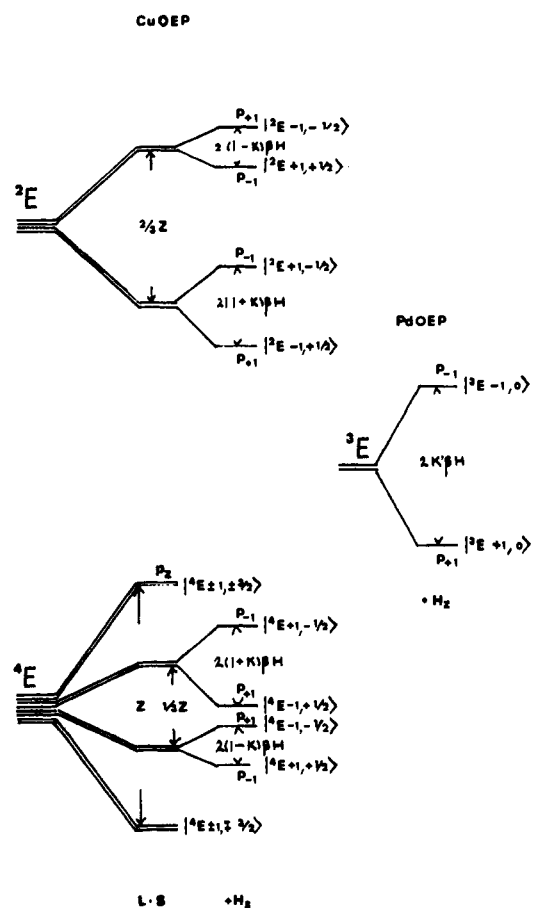


Figure 8. The splitting of the  ${}^2E$  and  ${}^4E$  levels of CuOEP by spin-orbit coupling and a magnetic field  $H_2$ .  $P \pm 1$  indicates the appropriate component of the electric dipole moment operator coupling the level to the ground state.

Figure 8 has been drawn up in a way to rationalize the observed spectra. It may be seen that a Boltzmann weighting of the lowest quartet emitting levels will give an opposite sign MCE from the  ${}^2E$  state, which in turn has the same sign as the signal from PdOEP. This, however, places certain restrictions on the reduced matrix elements  $z$  and  $K$ .  $K$  must be positive between 0 and 1, otherwise the  $|{}^4E + 1, +1/2\rangle$  and  $|{}^4E - 1, -1/2\rangle$  levels are inverted and would give the same sign MCE as the  $|{}^2E\rangle$  manifold. This value is sur-

Table II. The Vibrational Structure of CuOEP (Low-Temperature, 40-mW Laser)

Designation	Wavelength, Å	Energy, cm <sup>-1</sup>	Distance from 0-0, cm <sup>-1</sup>
0-0	6912	14468	
$\nu_1$	7020	14285	183
$\nu_2$	7156	13974	494
$\nu_3$	7264	13766	702

prisingly low. The experimentally determined value of  $K'$  for PdOEP is:

$$K' = \frac{i}{2^{1/2}} \langle e_g \| 1 \| e_g \rangle = 2.1$$

In addition, qualitative estimates of the value of  $K$  for CuOEP, judged from the spectra, indicate it to be a lot closer to 0 than 1. (Quantitative estimates are not possible, since the emission consists of overlapping transitions, and the temperature is uncertain.)

$z$  must be positive since otherwise the signs of the MCE of the doublet and quartet states would be inverted. Also,  $z$  must be sufficiently great to give the  $|^4E - 1, +\frac{1}{2}\rangle$  state a higher energy than the  $|^4E + 1, +\frac{1}{2}\rangle$  level. This implies the following inequality:

$$z > 6K\beta H_z$$

or

$$z > 5K \text{ cm}^{-1} \quad (10)$$

if the values of  $H_z$  and  $\beta$  are substituted. This is consistent with the estimates of Gouterman.<sup>11,31</sup>

We now turn to an investigation of the vibronic structure of CuOEP. Table II gives the energies of the various discernible peaks. In evolving his kinetic scheme, Gouterman chooses to regard the vibronics as a superposition of transitions from the doublet and quartet region, but does mention the possibility that the spectra could be interpreted in terms of a constant intensity quartet emission superimposed upon a temperature dependent emission from the <sup>2</sup>E level. Table IIIa gives the variation of the "band origin" energy with power, while Table IIIb gives the corresponding variation of the  $\nu_3$  vibration. Table IIIc gives the variation in the intensity of  $\nu_3$  with temperature, by normalizing with respect to amplification factors and laser power. Even allowing for errors in the estimation of the "position" of a broad band, and inaccurate measurement of the lower laser powers, there seems little doubt that the vibronics are based upon the quartet origin, and that the <sup>4</sup>E quantum efficiency is relatively independent of temperature over the region studied.

## Discussion

Perhaps the most important features to arise from the results of the last section are the small value of the reduced matrix element  $K$  in CuOEP, and the evidently large oscillator strengths of the vibrational side bands associated with the <sup>4</sup>E state. It is tempting to relate those two observations by invoking the Jahn-Teller effect, by analogy with the work of van der Waals<sup>18</sup> and Sutherland.<sup>16</sup> These workers have produced evidence for similar zero-field splittings of the <sup>1</sup>E state in zinc porphyrins contained in two totally different media. van der Waals specifically interprets his spectra in terms of a Jahn-Teller effect, and rationalizes his experimental results quite well by doing so.

Figure 9 indicates the nature of the potential energy surfaces of an E state split by a single Jahn-Teller active vibration ( $b_{1g}$  or  $b_{2g}$  in  $D_{4h}$ ). Two degenerate potential energy wells are formed, displaced by amounts  $\pm p_0$  along a nor-

Table III

Power, mW	Position, Å	Energy	Maximum energy shift
(a) Shift of Band Origin with Laser Power in CuOEP			
300	6856	14586	$\Delta E = 118 \text{ cm}^{-1}$
200	6864	14569	
100	6904	14484	
40	6912	14468	
(b) Shift of $\nu_3$ Vibration with Laser Power			
300	7240	13812	$\Delta E = 46 \text{ cm}^{-1}$
200	7240	13812	
100	7256	13782	
40	7264	13766	
(c) Normalized Height of $\nu_3$ at Different Laser Powers			
			Normalized height <sup>a</sup>
300			148
200			144
100			162
40			132

<sup>a</sup> The "normalized height" is in arbitrary units.

mal coordinate  $q$ .<sup>29</sup> The electronic wave functions of each surface are mutually orthogonal, and are simply the cartesian components  $E_x$ ,  $E_y$  of the distorted state. The displacements  $\pm p_0$  result in enhancement of the Franck-Condon factors for the vibrational side bands at the expense of that of the 0-0 transition, giving greater intensity to the former.

The effect on the  $L_z$  operator is as follows. The wave functions of the origin states are now vibronic ones:

$$\begin{aligned} \psi_1 + |^4E_x \Phi_1\rangle \\ \psi_2 + |^4E_y \Phi_2\rangle \end{aligned} \quad (11)$$

where  $\Phi_1$  and  $\Phi_2$  are vibrational wave functions for the displacement at  $-p_0$  and  $+p_0$ , respectively. Since the actual magnitude of the displacement  $p_0$  is thought to be rather small, the "crude adiabatic approximation" may be used. This gives:

$$\begin{aligned} \langle \psi_1 | L_z | \psi_2 \rangle = \langle ^4E_x | L_z | ^4E_y \rangle \langle \Phi_1 | \Phi_2 \rangle = \\ - \frac{1}{2^{1/2}} \langle e_g \| 1 \| e_g \rangle \langle \Phi_1 | \Phi_2 \rangle \end{aligned} \quad (12)$$

The overlap factor  $\langle \Phi_1 | \Phi_2 \rangle$  has been calculated by Wagner<sup>30</sup> assuming harmonic oscillator states. It is given by:

$$\langle \Phi_1 | \Phi_2 \rangle = e^{-S/2} [(S^m/m!)]^{1/2} \quad (13)$$

where  $m$  represents the quantum number of the vibronic state and  $S = 2\alpha^2 p_0^2$  is a measure of the strength of the coupling. The relationship with van der Waals' distortion parameter " $\alpha$ " is:

$$" \alpha " = (2S)^{1/2} \quad (14)$$

The actual magnitude of the reduced matrix element governing the magnetic-field splitting of the  $M = 0$  <sup>4</sup>E levels is then

$$\begin{aligned} K'' = + \frac{i}{2^{1/2}} \langle e_g \| 1 \| e_g \rangle e^{-S/2} \\ = K e^{-S/2} \end{aligned} \quad (15)$$

and is less than the undistorted value by  $e^{-S/2}$ . This is an example of a type of "one-dimensional Ham effect".

It is difficult to obtain more than a rough indication of the magnitude of the damping factor  $e^{-S/2}$ . If a mean estimate of  $K''$  of 0.5 is used and  $K$  is assumed to be around 3.5, from the work on absorption MCD, then  $e^{-S/2} = 0.14$ . A calculation of the damping factor of the <sup>1</sup>E state in zinc porphyrin, from the results of van der Waals, gives:

$$e^{-a^2/4} = 0.62$$

This leads to the tentative suggestion that the Jahn-Teller effect in the  ${}^4E$  state of CuOEP is abnormally large. The reasons for this are far from obvious. Nor is it clear why the quartet state should exhibit such an effect, while the nearby doublet state is quite "normal". The present experimental results give no hint of the answers.

Before leaving this aspect of the results, two more details may be mentioned. The spin-orbit coupling energies should be reduced by the same amount as the magnetic field shifts, since both processes involve interaction with the  $L_z$  operator. This means that  $z$  in eq 9 will be small, and that more powerful magnetic fields may be able to reverse the inequality in (10). This would either change the sign of the  ${}^4E$  MCE or possibly give it some "A" term character. It should certainly give a relative estimate of the magnitudes of "z" and "K".

The other striking features of the CuOEP emission are the relative insensitivity of the quantum efficiency of the  ${}^4E$  state to changes in temperature, and the absence of any MCE associated with the vibronic side bands. This first observation puts the kinetic scheme of Gouterman into doubt. However, the experiment described here is not suited to an investigation of the kinetics of the decay processes at present so an alternative scheme will not be discussed here. We hope to report the facility for time resolved MCE in due course.

The absence of any vibronic MCE is difficult to account for. If the side bands originated from transitions from the ground vibronic levels of the  ${}^4E$  surfaces, then they would be expected to have a similar MCE. This is, however, only an intuitive statement. The spin-forbidden nature of the transition, together with the possible excited state distortion and unknown vibrational symmetries, make the calculation of the vibronic MCE rather intractable. A possible rationalization of the absence of signal is that the transitions originate from the  $|{}^4E \pm 1 \pm 3/2\rangle$  level, and hence are  $z$  polarized. If this is the case, then it may be possible to explain the double lifetime phenomena. The  $M_s = \pm 3/2$  levels are expected to have much smaller oscillator strengths than the  $M_s \pm 1/2$  states (see earlier). If spin-lattice relaxations between the  $M_s \pm 1/2$  and  $M_s \pm 3/2$  levels were sufficiently slow, then the different states would be essentially uncoupled and radiate independently with different lifetimes. This effect is observed at very low temperatures (less than 4 K) with porphyrins in  $n$ -octane lattices, in which the spin-lattice coupling is expected to be much stronger than in a solution. More careful measurement of lifetime dependence with wavelength and luminescence polarization measurements may help to elucidate the problem.

## Conclusions

The data presented here indicate that the basic theoretical assumptions of Ake and Gouterman<sup>15,19</sup> are correct. The results for PdOEP indicate that the  ${}^3E$  state is substantially unaffected by the nature of the diamagnetic metal, and can be explained if spin-orbit coupling with allowed  ${}^1E_u$  states results in emission primarily from the  $|{}^3E \pm 1, 0\rangle$  levels. Strong support for the existence of "trip-doublet" and quartet levels, with the doublet approximately 100  $\text{cm}^{-1}$  to higher energy than the quartet, is provided by the MCE of CuOEP. However, the quartet state appears to be affected by a strong Jahn-Teller distortion, significantly, quenching the orbital angular momentum. The nature of the radiative and nonradiative decay processes are also more complicated than suspected by Gouterman. The results are compatible with the work of van der Waals et al. on the zinc porphyrin system in  $n$ -octane single crystals.

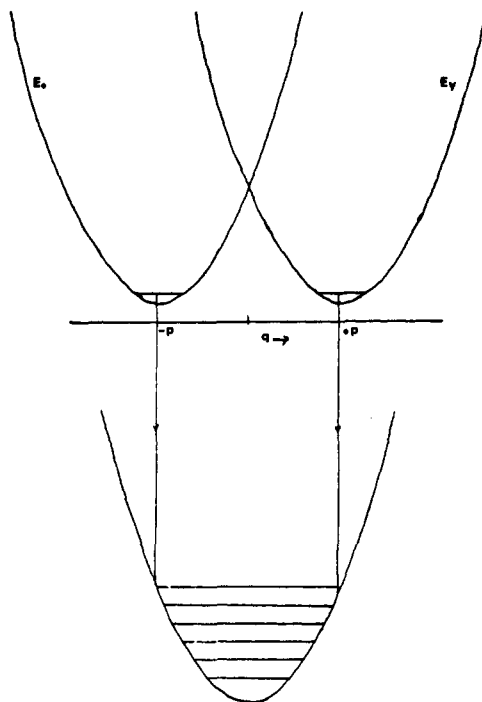


Figure 9. The effect of a Jahn-Teller distortion on an E state in  $D_{4h}$ .

However, the magnitude of the distortion of the  ${}^4E$  state in CuOEP seems to be much larger than that found by these workers in the  ${}^1E_u$  state of ZnP. The reasons for this are not clear.

More accurate temperature measurements are required before quantitative information on the vibronic interaction in these systems is obtained. In particular, work with strong magnetic fields and an immersion system should prove profitable in the elucidation of the problems associated with CuOEP.

**Acknowledgment.** We wish to thank the Science Research Council for graduate studentships (R.A.S.) (R.G.) and for financial support of this project.

## Appendix

**An Outline of the Moments Theory Suitable for Treatment of the MCE Results on the Porphyrins.** In the porphyrins we need to consider the case of transitions from an excited state manifold  $|a_0\rangle \in A$  to a ground state manifold  $|b\rangle \in B$ . The energy levels in both the ground and excited state are broadened by interactions with the solvent. It is assumed that both the solvent interactions and the perturbations induced by the magnetic field act only within each degenerate electronic manifold and do not couple electronic states of different energies. In this case the "average energy theorem" of Henry and Slichter applies, i.e., the shift of line shape due to magnetic interactions is independent of the magnitude of the solvent-molecule perturbations, and may consequently be treated in terms of a basis set describing the isolated molecule. If, in addition, this basis set is made diagonal in  $M_J$ , then the expressions for the average energy shift become particularly simple.

The emission intensity of transitions between the two manifolds is represented by:

$$I^i(\nu) \propto \sum_{A \rightarrow B} N_i \nu^4 |\langle a_i | P^m | b_j \rangle|^2 \delta(\nu_{aibj} - \nu) \quad (1)$$

where  $i$  and  $j$  run over the perturbed levels of the excited and ground states, respectively.  $N_i$  is the population of the  $|a_i\rangle$  level.

The signal detected by the instrument is  $I_{A \rightarrow B}(v)$  multiplied by an instrumental response function  $G(v)$ . The ac and dc components are given by:

$$S(v)_{ac} = G(v) \sum_{i,j} N_i v^4 (\Delta P_{ij}) \delta(v_{ij} - v)$$

$$S(v)_{dc} = G(v) \sum_{i,j} N_i v^4 P_{ij} \delta(v_{ij} - v) \quad (2)$$

where

$$\Delta P_{ij} = |\langle a_i | P^+ | b_j \rangle|^2 - |\langle a_i | P^- | b_j \rangle|^2$$

$$P_{ij} = |\langle a_i | P^+ | b_j \rangle|^2 + |\langle a_i | P^- | b_j \rangle|^2 \quad (3)$$

The  $S(v)$  are thus the products of two frequency dependent functions. Ideally, the instrument response function should be known in order to extract information about the "molecular response function". However, except in the case of very broad bands, it will not be too bad an approximation to take a mean value over the emission profile.

The zeroth moment of the emission may now be defined as:

$$\langle F_0 \rangle = \int_{\text{band}} \frac{S(v)_{ac}}{v^4} dv / \int \frac{S(v)_{dc}}{v^4} dv \quad (4)$$

From (2)

$$\langle F_0 \rangle = \sum_{i,j} N_i \Delta P_{ij} / \sum_{i,j} N_i P_{ij} \quad (5)$$

From now on, the procedure followed is very similar to that adopted by Stephens<sup>13</sup> and Henry et al.<sup>12</sup> and will not be repeated here. The  $N_i$  are approximated by the first two terms in a Boltzmann expansion, and the  $a_i$  and  $b_j$  are expressed in terms of complete sets of unperturbed basis functions. By a combination of orthogonality conditions, closure relationships, and time reversal symmetry, the solvent perturbations are eliminated from the expression for the numerator in (5). The elimination of solvent and field effects from the denominator is by less rigorous methods. Field effects are disregarded by the experimental observation that the emission spectrum changes insignificantly upon application of a magnetic field. In order to disregard the solvent perturbations from this term one has to make the assumption that the oscillator strength does not change significantly in going from a free, isolated molecule to the solution. While this is probably a reasonable assumption in the case of the comparatively large oscillator strengths dealt with in absorption, the same is not necessarily true for the weak forbidden transitions studied in emission. There is no simple way of checking the validity of this assumption, other than by lifetime measurements in the gas phase. The phosphorescent lifetimes of many porphyrins are relatively solvent independent (assuming the latter to be nonpolar), which is some justification for the approximation. Nevertheless, this must remain a more dubious step to make than the equivalent one in absorption theory.

The final expression for the zeroth moment is

$$\langle F_0 \rangle = \frac{1}{KT} \frac{\sum_{a_0 b_0} \Delta P_{a_0 b_0} \langle a_0 | H_0^m | a_0 \rangle}{\sum_{a_0 b_0} P_{a_0 b_0}} \quad (6)$$

where  $H_0^m = -8H_z(L_z + 2S_z)$  and  $a_0$  and  $b_0$  are the unperturbed basis functions of the excited and ground states.

Equation 6 assumes the space and molecular fixed axes to be equivalent. In an isotropic solvent this is not the case. Orientational averaging may be performed by the methods outlined by Edmonds. The denominator contains terms  $|\langle a_0 | P^m | b_0 \rangle|^2$ . If the space and molecular fixed axes are con-

nected by a unitary transformation, and if the operators are proportional to spherical harmonics, then

$$P^n = \sum_i D_{i,n}^{(i)}(\omega) P^i \quad (7)$$

where  $P^n$  is in the space fixed system, and  $D_{i,n}^{(i)}(\omega)$  is the first rank rotation matrix connecting the space and molecular fixed axes. The  $a_0$  and  $b_0$  are defined in the molecular framework, so:

$$|\langle a_0 | P^m | b_0 \rangle|^2 = \langle a_0 | P^m | b_0 \rangle \langle b_0 | P^{m*} | a_0 \rangle = \sum_{i,i'} D_{i,n}^{(i)}(\omega) D_{i',n}^{(i)*}(\omega) \langle a_0 | P^i | b_0 \rangle \langle b_0 | P^{i*} | a_0 \rangle \quad (8)$$

Orientational averaging involves integration over the Euler angles. See Edmonds, for the appropriate integrals. Thus

$$\overline{|\langle a_0 | P^m | b_0 \rangle|^2} = \sum_{i,i'} \delta_{i,i'} \frac{1}{3} |\langle a_0 | P^i | b_0 \rangle|^2 \quad (9)$$

The average of the denominator of (6) is then given by:

$$\frac{2}{3} \sum_{a_0 b_0} |\langle a_0 | P^i | b_0 \rangle|^2 \quad (10)$$

An important point to note is that the index  $i$  may run from  $-1, 0, +1$ , thus "z" polarized transitions may contribute to the emission intensity. The first term under the sum in the numerator is:

$$\langle a_0 | H_0^m | a_0 \rangle \langle a_0 | P^+ | b_0 \rangle \langle b_0 | P^- | a_0 \rangle \quad (11)$$

In transforming solely to the molecular axes this gives:

$$\sum_j D_{j,0}^{(i)}(\omega) D_{1+1}^{(i)}(\omega) D_{1-1}^{(i)}(\omega) \times \langle a_0 | H_3^m | a_0 \rangle \langle a_0 | P^i | b_0 \rangle \langle b_0 | P^i | a_0 \rangle \quad (12)$$

Upon averaging this becomes:

$$\sum_j \left( \begin{matrix} j & i & i' \\ j & 1 & -1 \end{matrix} \right) \left( \begin{matrix} 1 & 1 & 1 \\ 0 & +1 & -1 \end{matrix} \right) \langle a_0 | H_j^m | a_0 \rangle \langle a_0 | P^i | b_0 \rangle \langle b_0 | P^i | a_0 \rangle \quad (13)$$

Since the  $a_0$  are diagonal in  $L_z$ ,  $j = 0$ , and so  $i' = -1$ . Also  $i = 0$  since the  $3 - j$  symbol is then zero. Now

$$\left( \begin{matrix} 1 & 1 & 1 \\ 0 & +1 & -1 \end{matrix} \right) = \frac{1}{6^{1/2}} \text{ and } \left( \begin{matrix} 1 & 1 & 1 \\ 0 & -1 & +1 \end{matrix} \right) = -\frac{1}{6^{1/2}}$$

So (13) becomes

$$\frac{1}{6} \langle a_0 | H_0^m | a_0 \rangle |\langle a_0 | P^+ | b_0 \rangle|^2 - |\langle a_0 | P^- | b_0 \rangle|^2 \quad (14)$$

Similarly, the second term under the sum in the numerator of (6) is

$$\frac{1}{6} \langle a_0 | H_0^m | a_0 \rangle \{ |\langle a_0 | P^- | b_0 \rangle|^2 - |\langle a_0 | P^+ | b_0 \rangle|^2 \} \quad (15)$$

Hence the final expression for the rotationally averaged zeroth moment is

$$\langle F_0 \rangle = \frac{1}{2KT} \times \frac{\sum_{a_0 b_0} \langle a_0 | H_0^m | a_0 \rangle \{ |\langle a_0 | P^+ | b_0 \rangle|^2 - |\langle a_0 | P^- | b_0 \rangle|^2 \}}{\sum_{a_0 b_0} |\langle a_0 | P^i | b_0 \rangle|^2} \quad (16)$$

## References and Notes

- (1) R. A. Shatwell and A. J. McCaffery, *J. Chem. Soc., Chem. Commun.*, 546 (1973).



- (2) J. B. Allison and R. S. Becker, *J. Chem. Phys.*, **32**, 1410 (1960).  
 (3) P. G. Seybold and M. Gouterman, *J. Mol. Spectrosc.*, **31**, 1 (1964).  
 (4) R. A. Shatwell and A. J. McCaffery, *Phys. Rev. B*, in press.  
 (5) A. J. McCaffery and R. A. Shatwell, *Mol. Phys.*, to be published.  
 (6) A. J. McCaffery, P. Brint, R. Gale, and R. A. Shatwell, *Chem. Phys. Lett.*, **22**, 600 (1973).  
 (7) R. A. Shatwell and A. J. McCaffery, *J. Phys. E*, **7**, 297 (1973).  
 (8) P. N. Schatz and A. J. McCaffery, *Q. Rev., Chem. Soc.*, **552** (1969).  
 (9) J. Falk, "Porphyrins and Metalloporphyrins", Elsevier, New York, N.Y., 1964.  
 (10) D. Eastwood and M. Gouterman, *J. Mol. Spectrosc.*, **35**, 359 (1970).  
 (11) M. Gouterman, R. A. Mathias, B. E. Smith, and W. S. Caughey, *J. Chem. Phys.*, **52**, 3795 (1970).  
 (12) C. H. Henry, S. E. Schnatterly, and C. P. Schlichter, *Phys. Rev.*, **137**, 583 (1965).  
 (13) P. J. Stephens, *J. Chem. Phys.*, **52**, 3489 (1970).  
 (14) M. Gouterman, *J. Chem. Phys.*, **30**, 1139 (1959).  
 (15) R. L. Ake and M. Gouterman, *Theor. Chim. Acta*, **15**, 20 (1969).  
 (16) R. L. Sutherland, D. Axelrod, and M. A. Klein, *J. Chem. Phys.*, **54**, 2888 (1971).  
 (17) A. T. Gradyushko et al., *Biofizika*, **14**, 827 (1969).  
 (18) G. Canters, J. van Egmond, T. J. Schaafsma, and J. van der Waals, *Mol. Phys.*, **24**, 1203 (1972).  
 (19) (a) R. L. Ake, Ph.D. Thesis, Harvard, 1968; (b) R. L. Ake and M. Gouterman, *Theor. Chim. Acta*, **17**, 408 (1970).  
 (20) J. N. Murrell, *Mol. Phys.*, **3**, 319 (1960).  
 (21) B. E. Smith and M. Gouterman, *Chem. Phys. Lett.*, **2**, 517 (1968).  
 (22) J. S. Griffith, "The Irreducible Tensor Method for Molecular Symmetry Groups", Prentice-Hall, Englewood Cliffs, N.J., 1962.  
 (23) G. P. Gurinovich, A. N. Sevechenko and K. N. Solovov, Ed., "Spectroscopy of Chlorophyll and Related Compounds", Minsk, 1968.  
 (24) P. J. Stephens, W. Suetaka, and P. N. Schatz, *J. Chem. Phys.*, **44**, 4592 (1966).  
 (25) R. Gale, A. J. McCaffery, and M. D. Rowe, *J. Chem. Soc., Dalton Trans.*, 596 (1972).  
 (26) G. McHugh, M. Gouterman, and C. Weiss, *Theor. Chim. Acta*, **24**, 346 (1972).  
 (27) Results from Ph.D. Thesis of Dratz, quoted in ref. 15.  
 (28) J. Nestor and T. G. Spiro, *J. Raman Spectrosc.*, **1**, 539 (1973).  
 (29) J. T. Hougen, *J. Mol. Spectrosc.*, **13**, 149 (1964).  
 (30) M. Wagner, *J. Chem. Phys.*, **41**, 3939 (1964).  
 (31) A referee has suggested an alternative interpretation for the MCE results on CuOEP. This is that the peak at 6912 Å is from the trip-doublet ( ${}^2T_1$ ) designated  ${}^2E_u$  in our text while the 6820 Å signal arises from the second trip-doublet ( ${}^2T_2$ ) arising from coupling with the B state triplet and thought also to be in this energy region.<sup>12</sup> Field-induced mixing of these states might show similar effects to those observed. We do not pursue this argument here but hope to clarify this question in a future publication describing MCE results on CuOEP at temperatures below 4.2 K

## A Dynamic Nuclear Magnetic Resonance Study of Fluorine Exchange in Liquid Sulfur Tetrafluoride<sup>1</sup>

Walter G. Klemperer,\*<sup>2a</sup> Jeanne K. Krieger, Michael D. McCreary,  
 E. L. Muettterties,\*<sup>2b</sup> Daniel D. Traficante, and George M. Whitesides\*<sup>2c</sup>

Contribution from the Departments of Chemistry, Massachusetts Institute of Technology, Cambridge, Massachusetts 02139, and Cornell University, Ithaca, New York 14850. Received April 7, 1975

**Abstract:** The temperature dependence of the NMR spectrum of SF<sub>4</sub> has been reexamined, and the observed line shapes in the region of intermediate exchange compared with theoretical line shapes calculated for a number of different methods of permuting axial and equatorial fluorine atoms. Carefully purified SF<sub>4</sub> yields experimental spectra in good agreement with those calculated assuming the intramolecular fluorine exchange characteristic of Berry pseudorotation; these experimental spectra do not closely resemble those calculated on the basis of any intermolecular permutation we have examined. The exchange rate in unpurified SF<sub>4</sub> is substantially higher than in carefully purified material. The line shapes observed for unpurified material can be matched to those calculated assuming permutations characteristic of several plausible bimolecular mechanisms; available data do not uniquely define the mechanism of this impurity-catalyzed exchange.

At low temperatures, liquid SF<sub>4</sub> displays an A<sub>2</sub>B<sub>2</sub> NMR spectrum characteristic of a C<sub>2v</sub> molecule;<sup>3</sup> as the temperature is raised, fluorine site exchange leads to line broadening and eventual coalescence to a single sharp resonance.<sup>3</sup> This spectral temperature dependence has been extensively examined, but a unique mechanistic interpretation of this dependence has proved elusive. In 1958, Cotton, George, and Waugh<sup>4</sup> surmised that fluoride impurities induced fluorine exchange in their substantially contaminated samples. Muettterties and Phillips<sup>5</sup> subsequently published similar spectra, and, noting a dependence of fluorine exchange rate on sample concentration, advocated intermolecular mechanisms involving dimeric or ionic intermediates. In a later publication,<sup>6</sup> however, they emphasized the possibility that traces of HF might be catalyzing fluorine exchange and also expressed the belief that intramolecular exchange does occur, but at a rate lower than the observed higher-order processes. The hypothesis of impurity catalysis was supported by Bacon, Gillespie, and Quail,<sup>7</sup> and more recently by Gibson, Abbott, and Janzen,<sup>8</sup> who retarded the rate of fluorine exchange by careful sample purification. The latter authors, however, were unable to establish that all impurities had been removed.

Other physical studies of sulfur tetrafluoride have failed to clarify the relative importance of intra- and intermolecular paths for the fluorine exchange. Redington and coworkers strongly favored bimolecular mechanisms on the basis of matrix-isolation infrared spectra,<sup>9,10</sup> and variations in NMR coupling constants and chemical shifts with medium have been interpreted as indicating intermolecular association of liquid SF<sub>4</sub>.<sup>11</sup> Gas phase studies, employing both far-infrared spectroscopy<sup>12</sup> and electron diffraction,<sup>13</sup> implicated intramolecular exchange processes. Theoretical studies<sup>14,15</sup> also propose intramolecular exchange in the gas phase, thus lending credence to Muettterties and Phillips' hypothesis that intramolecular exchange might be observed in the liquid phase if higher-order processes could be suppressed.

The present dynamic NMR study was undertaken to delineate the site exchange scheme responsible for fluorine exchange in sulfur tetrafluoride, and thus unambiguously determine which, if any, of the proposed exchange mechanisms are consistent with experiments. The results of this investigation are reported in three parts: (i) generation of all possible site exchange schemes implied by intramolecular, impurity catalyzed, and bimolecular mechanisms,